npg

Diverse system stresses: common mechanisms of chromosome fragmentation

JB Stevens[1], BY Abdallah[1], G Liu[1], CJ Ye[2], SD Horne[1], G Wang[1], S Savasan[3], M Shekhar[4], SA Krawetz[1], M Hüttemann[1], MA Tainsky[4], GS Wu[3], Y Xie[3], K Zhang[1] and HHQ Heng*,[1,3,4]

Chromosome fragmentation (C-Frag) is a newly identified MCD (mitotic cell death), distinct from apoptosis and MC (mitotic catastrophe). As different molecular mechanisms can induce C-Frag, we hypothesize that the general mechanism of its induction is a system response to cellular stress. A clear link between C-Frag and diverse system stresses generated from an array of molecular mechanisms is shown. Centrosome amplification, which is also linked to diverse mechanisms of stress, is shown to occur in association with C-Frag. This led to a new model showing that diverse stresses induce common, MCD. Specifically, different cellular stresses target the integral chromosomal machinery, leading to system instability and triggering of MCD by C-Frag. This model of stress-induced cell death is also applicable to other types of cell death. The current study solves the previously confusing relationship between the diverse molecular mechanisms of chromosome pulverization, suggesting that incomplete C-Frag could serve as the initial event responsible for forms of genome chaos including chromothripsis. In addition, multiple cell death types are shown to coexist with C-Frag and it is more dominant than apoptosis at lower drug concentrations. Together, this study suggests that cell death is a diverse group of highly heterogeneous events that are linked to stress-induced system instability and evolutionary potential.

Cellular stress has been implicated in many diseases, including cancer. During cancer progression, cellular stress promotes adaptive genome alterations, which increase the probability of somatic evolution.[1] Multiple types of stress have been documented occurring through various molecular mechanisms, and some are linked to genome instability and apoptosis.[2,3] However, cell death occurs in a number of forms, and apoptosis does not adequately represent the amount of cell death that happens in tumors in response to chemotherapy or radiation.[4] Apoptosis tends to occur in response to relatively high levels of drug treatment, often higher than clinical levels,[5] and the exact functions of apoptotic proteins can be contextually dependent. For example, in some cases activation of apoptotic proteins may drive proliferation. Furthermore, tumor cells often overexpress antiapoptotic proteins or lack intact cell-cycle checkpoints.[6] Loss of checkpoint function allows the cells to progress to mitosis despite the presence of damaged DNA, often resulting in mitotic cell death (MCD).

Although MCD accounts for the majority of tumor cell death during treatment, its mechanism(s) is largely unknown.[5,7–9] MCD appears as at least two major phenotypes: One is mitosis associated cell death, which occurs following abnormal segregation, where death takes place in G_1 following abnormal division. This form of MCD is associated with classical apoptosis, as the caspase cascade is activated following entry of multinucleated cells into G_1, and is referred to as mitotic catastrophe (MC).[9,10] Another is chromosome fragmentation (C-Frag) that occurs directly during mitosis. It is readily identifiable in cytogenomic figures where degraded chromosomes are evident.[9]

To illustrate the basis of C-Frag, many diverse stresses leading to C-Frag are analyzed. A simple relationship between diverse system stresses and C-Frag is established. These stresses are shown to converge on the induction of centrosome amplification, a major component in the regulation of genome stability. Based on this relationship, the common mechanism of cell death is re-synthesized: (1) Cell death is a general response of the cellular system to stress, having a role in rebalancing the cellular system. C-Frag, a main phenotype of MCD, is achieved through an array of individual molecular mechanisms, including centrosome amplification. (2) The type of cell death that will dominate in a given sample is dependent on multiple factors, including the availability of both the targets in cells (checkpoint function, whether cells are actively dividing) and the specifics of drug treatment. (3) The types of cell death induced are heterogeneous, as shown by cytogenomic analysis. Such heterogeneity, in addition to

genome-level heterogeneity,[11,12] explains why drug treatment can favor cancer evolution, as treatment induces stress leading to genome-mediated cancer evolution.[1,13] Recent reports have detailed processes where cassettes of fragmented chromosomes have been rejoined to form highly recombined chromosomes.[11,14,15] This process can affect a small number of chromosomes or nearly the entire genome, resulting in the induction of genomic instability, formation of new genome systems, and providing material for genome-based cancer evolution. Owing to the associations between C-Frag, genomic instability, disease progression, and the intervention of chemotherapies, this work underscores the potential of using C-Frag as a diagnostic tool in clinical settings.

Results

Realizing the underlying complexity of cell death processes, we have attempted to use multiple, diverse systems in order to determine the common mechanism(s) of C-Frag, which contrasts the traditional approach of using the same system to study different aspects.

PARP cleavage is associated with C-Frag. In multiple forms of cell death, DNA is degraded before stores of ATP are depleted; however, proteins such as PARP could repair the degrading DNA.[16] DNA repair is avoided through the degradation of PARP by a broad range of proteases.[16] Therefore, PARP cleavage was analyzed during the process of C-Frag and PARP was readily degraded (Figure 1a).

C-Frag differs from MC. To compare MC and C-Frag, a well-described model of MC was analyzed for C-Frag.[17] Cytogenomic analysis shows that, in contrast to previous reports, the mitotic fraction of cells actually decreases, suggesting that this form of MC is not mitotic in origin (Figure 1b). During treatment cells became enlarged (Figure 1c) and began to die. Over the course of treatment, the frequency of C-Frag did increase, but not enough to account for the amount of cell death previously reported, showing the difference between C-Frag and MC (Figure 1b). Previous studies have focused on the G2/M based on DNA content alone.[17] It is thus possible that the death observed previously was associated with cells in G2. The main morphologies observed during MC include apoptotic cells, multinucleated cells, and cells undergoing C-Frag (Figure 1d).

G_2 checkpoint abrogation through loss or reduction of gene function may result in increased C-Frag. UCN-01, which ameliorates G_2 checkpoint function, has a cooperative effect with many other chemotherapeutics, likely through induction of mitotic death.[18] To determine whether this death is correlated with C-Frag, HCT116 cells were treated with UCN-01 and doxorubicin (Dox). Treatment resulted in the
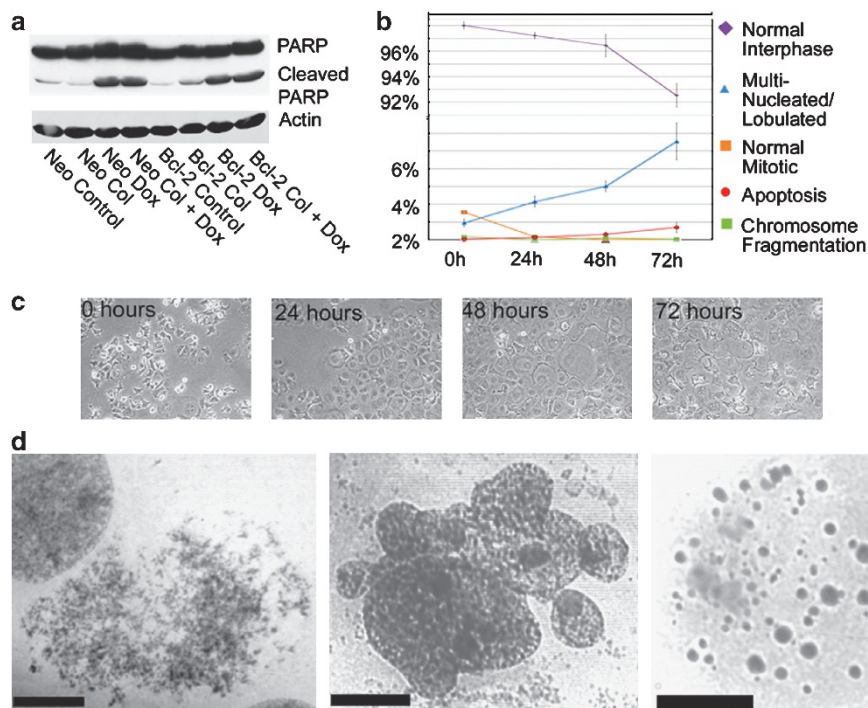
Figure 1 (**a**) Induction of C-Frag in H460-neo- and H460-Bcl-2-overexpressing cells by concurrent 12-h treatment with colcemid and Dox results in complete cleavage of PARP. Bcl-2-overexpressing and control cells were used to show that PARP degradation is not caused by apoptotic death in the case of C-Frag. (**b–d**) HCT116 14-3-3$\sigma^{-/-}$ cells treated with 0.2 μg/ml Dox have been shown to die through MC.[17] Seventy-two hours of treatment results in the mitotic index falling to almost 0 (orange line), whereas the percentage of multi-nucleated/multi-lobulated cells increases significantly (blue line) and the percentage of apoptotic cells rises slightly (red line) (**b**). During this time there is a degradation of cellular morphology as cells enlarge and die, and in agreement with previous results, by 72 h approximately 90% of cells died (**c**).[17] In previous reports, the bulk of cell death was thought to be occurring in mitotic cells; however, we were unable to identify such population by cytogenomic analysis, suggesting that this death may not be attributable to mitosis. (**d**) Examples of C-Frag, apoptotic, and multi-lobulated/nucleated cells are shown on the left, the middle, and the right, respectively following conventional cytogenetic preparation

Figure 2 C-Frag is detectable in *in vivo* tumors prepared for cytogenomic analysis (**a**). Here, two examples of cells undergoing C-Frag from an untreated primary mouse tumor are shown (left and right panels). In the photo on the right the cell on the top left is an example of a defective mitotic figure (DMF) that is also undergoing C-Frag.[12] The morphology of C-Frag is readily distinguishable from the normal mitotic figures of the same tumor (**b**)
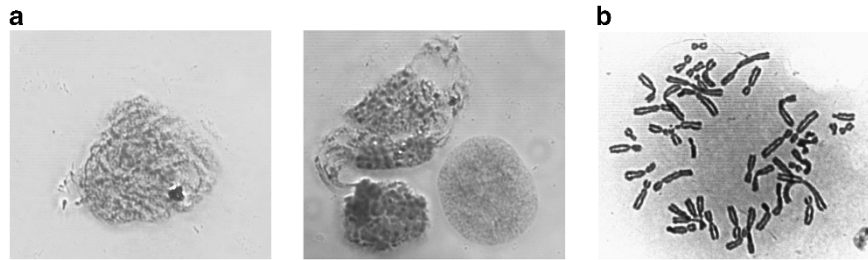
induction of C-Frag in 36.3% of mitotic cells following 300 nM UCN-01 and 1 μg/ml Dox treatment for 6 h. By contrast, cells treated with UCN-01 or Dox alone showed a C-Frag index (CFI) of 7.2 and 9.4%, respectively, showing that abnormal passage of damaged cells from G_2 to mitosis can result in C-Frag.

Clinical relevance of C-Frag. C-Frag was mainly characterized using *in vitro* cell culture models.[9] C-Frag was detected in mouse xenograft tumors without culture. C-Frag (Figure 2a) is distinguishable from normal mitotic cells (Figure 2b). We next determined the potential clinical utility of C-Frag. Tumors were analyzed from a number of cancer types, including short-term cultured solid tumors and peripheral lymphocytes from patients with hematological malignancies, and C-Frag was found to occur in all the samples (Stevens *et al.*, unpublished data).

Linking C-Frag to various types of stresses. According to the genome theory,[1,11–13,19,20] genome system instability can be induced by various stresses, including disease conditions; we thus hypothesize that system stress might represent the underlying mechanism of C-Frag. Both internal and induced stresses were examined using diverse experimental systems.

Genomic instability leads to C-Frag. C-Frag was monitored in the early and late stages of a model of spontaneous *in vitro* immortalization (MDAH-041) and mouse ovarian surface epithelial cell (MOSEC) model progression.[11,13] In the MDAH-041 model, the spontaneous C-Frag index (CFI) mirrors overall genomic instability as measured by non-clonal chromosome aberrations (NCCAs). The CFI is 6% at pd25, whereas once the cells stabilize at pd54 the CFI falls to 2.9% (Figure 3a). In the MOSEC model, early-stage (p9) cells have high levels of genomic instability, whereas at later stages (p91) the cells become more clonal.[13] In the early stages, these cells had a moderate frequency of spontaneous C-Frag (8.8%), whereas in the late stable stages this reduced to 0.8%. Genomic instability is linked to the generation of C-Frag.

Culture stress induces C-Frag. C-Frag was first analyzed in response to temperature changes. COLO-357 cells were cultured at 37°C and then shifted to 42°C for 2 weeks before being switched back to 37°C (Figure 3b). When shifted from 37 to 42°C, the cells showed an increase in CFI within 24 h of shifting ($P < 0.01$). The CFI stabilized at < 6% within 120 h of the switch. The cells stabilized at 42°C were switched back to 37°C and showed an increase in the CFI ($P = 0.042$) until it

fell to < 5% within 120 h. The observation that switching cells stabilized at 42°C back to the 'normal' temperature of 37°C induces C-Frag is significant. It suggests that any change to the current system status is a key source of stress, and that cell death is one mechanism of system adaptation.

Most cell culture uses atmospheric oxygen concentrations (20%), whereas *in vivo* cells rarely experience over 3.5% O_2.[21] HCT116 cells were acclimated for 5 days to 3.5% oxygen. For the first 3–4 days population doubling slowed or stopped, until cells began to once again cycle regularly. Concurrent treatment of these acclimatized cells with Dox and colcemid resulted in a CFI of 54.7%, which is lower than the typically observed CFIs for HCT116 cells (nearly 100%) with the same treatment at atmospheric oxygen. Thus, similar to other forms of programmed cell death,[21] a normoxic environment suppresses C-Frag as compared with a hyperoxic environment.

ER stress induces C-Frag. Multiple pathways regulate various endoplasmic reticulum (ER) stress response pathways, including calcium stress, unfolded protein response, and oxidative stress.[22] To determine whether these specific stress pathways could lead to C-Frag, COLO-357 cells were treated with various inducers of ER stress. Treatment with dithiothreitol (DTT), which induces the unfolded protein response by interfering with protein folding, strongly induced C-Frag (Figure 3c). Treatment with thapsigargin (TG) and tunicamycin (TM) also increased the CFI, whereas A23187 did not, instead completely blocking entry into mitosis. All four drugs induced the unfolded protein response (Figure 3d). The differential frequencies of C-Frag and apoptosis between these treatments suggest that the type of cell death depends on the availability of the targets, as with A23187 treatment there were no mitotic cells providing material for C-Frag.

Inhibition of HSP90 increases chromosome fragmentation. Heat-shock proteins (HSPs) respond to cellular stress and HSP90 specifically functions in a multitude of stress pathways. To determine whether HSP90 function may have a role in C-Frag, cells were cultured using varying concentrations of Dox that would arrest the cell-cycle and deplete mitotic cells required for C-Frag. The cells were then treated with 17-DMAG (water-soluble geldanamycin analog), a potent HSP90 inhibitor. This resulted in an increase in the frequency of C-Frag (Figure 3g), indicating that inhibition of major stress pathways predisposes cells to death.
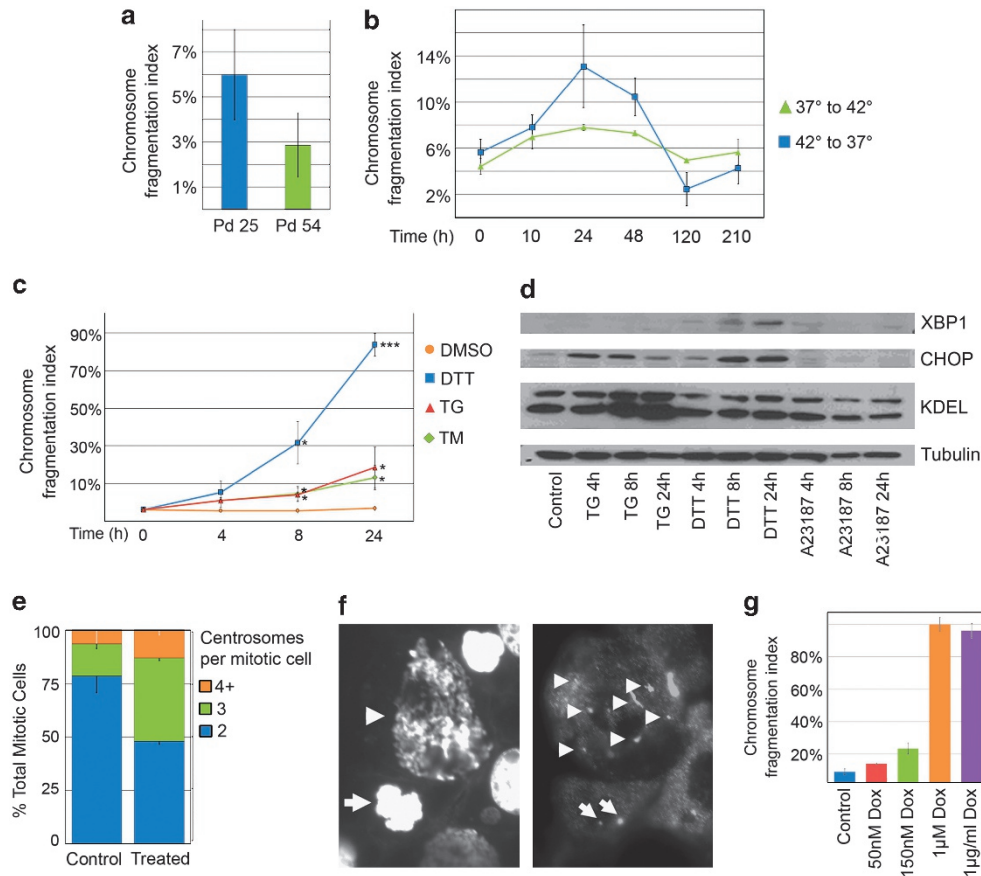
Figure 3 The effects of various stressors on C-Frag are examined ($*P<0.05$, $**P<0.01$, $***P<0.001$) (a–c). (a) C-Frag is elevated during genomic instability (pd25) (blue bar) as compared with stable genomes (pd54) (green bar, $P<0.05$). (b) Increasing the culture temperature of COLO-357 cells from 37 to 42°C (blue line) results in a transient increase in the frequency of C-Frag until spontaneous C-Frag falls to $>6\%$. Following the shift of temperature back to 37°C (green line) there is another corresponding increase in the CFI, which then stabilizes at $<5\%$. Statistical significance was calculated by comparing each time point to the 0 time point of the treatment. (c) Treatment of COLO-357 cells with specific stress inducers, including DTT (blue line), TG (red line), and TM (green line), results in varied increased C-Frag over a 24-h period. The error bars represent the standard deviation. (d) Western blot analysis of the same DTT and TG treatments show an increase in the expression of CHOP, a key protein in the ER stress response. CHOP expression increases steadily in both TG and DTT treatments from 0 to 8 h, then falls off at 24 h as cells adapt to the stress. Activated XBP1 expression changes similarly in DTT-treated cells, whereas TG treatment results in little expression. Finally, there is an increase in ER proteins bearing the ER translocation sequence KDEL from 0 to 24 h of treatment, which is indicative of ER stress (d). Concurrent treatment with colcemid and Dox to induce C-Frag in HCT116 cells results in increased centrosome amplification (e). (f) An example of centrosome amplification (right panel, arrowheads) taking place in a cell undergoing C-Frag (left panel, arrowhead). Multiple centrosomes are detectable (arrowheads), whereas in a normal neighboring cell undergoing mitosis (left panel, arrow), only two centrosomes are present (right panel, arrows). Inhibition of HSP90 function with 17-DMAG results in increased C-Frag (g). Bars represent the CFI of cells treated with or without (control – blue bar) doxorubicin at the indicated concentration for 54 h. After 24 h of treatment 100 nM 17-DMAG was added followed by the addition of colcemid 6 h prior to harvest. Doxorubicin treatment at 1 µM and 1 µg/ml (orange and purple bars respectively) would typically result in cell cycle arrest and death via apoptosis or necrosis, however 17-DMAG treatment allows cells to progress to mitosis with damage. Damaged mitotic cells are then eliminated by C-Frag. Treatment with 50 nM (red bar) and 150 nM (green bar) elevates the CFI, however many cells do not contain sufficient damage to induce C-Frag

Centrosome amplification occurs in cells treated to undergo C-Frag. Centrosome amplification has been linked to temperature stress-induced MCD.[23] Association of centrosome amplification with C-Frag may help to elucidate its mechanisms. In non-treated HCT116 cells, 21.3% of mitotic cells show three or more centrosomes (Figures 3e and f). By contrast, cells treated concurrently for 12 h with colcemid and 1 µg/ml Dox showed centrosome amplification in 51.7% of mitotic cells ($P=0.021$). Furthermore, $ATM^{-/-}$ mouse cells were shown previously to exhibit centrosome amplification.[24] C-Frag was found to be present in embryonic fibroblasts and lymphocytes from these mice (data not shown). Thus, there is linkage between abnormal centrosome counts and increased C-Frag.

HSP90 is a core centrosome component, suppresses centrosome instability, and is linked to MCD.[25] In addition to observing increased centrosome amplification during C-Frag, it increased in association with HSP90 inhibition. Centrosome instability is also associated with genomic instability, a form of system stress that is capable of inducing C-Frag. It is thus likely that centrosome amplification is a response to stress and mechanistically links stress to MCD.

The relationship between C-Frag and other types of cell death. ER stress has been previously linked to cell death by apoptosis. Our current study also links ER stress to C-Frag; however, C-Frag and apoptosis likely use different mechanisms.[9] Traditional studies focus on one type of cell

Table 1 Nuclear features of types of cell death

Type of death	Cytogenomic features
Apoptosis	Nuclear blebbing resulting in grape-like clusters
Necrosis	Nuclear shrinkage (pyknosis)
Autophagy	Little if any change in nuclear morphology
Chromosome fragmentation	Degradation of condensed mitotic chromosomes

Figure 4 Different treatment combinations result in different outcomes. Concurrent treatment of HCT116 cells with colcemid and Dox, mitomycin-C (MMC), or methotrexate (MTX) result in a varied induction of cell death by apoptosis (green bars) and C-Frag (blue bars) as judged by cytogenetic examination (**a**). Treatment of cells with docetaxel instead of colcemid results in mitotic arrest as expected, combinatorial treatment with 1 μg/ml Dox and either 1 μM docetaxel or 10 μM docetaxel results primarily in C-Frag or apoptosis, respectively (**b**). As judged by previous work, some of the values for apoptotic death observed here were lower than what has been shown previously. This is likely because of differences in cytogenomic assays as compared with molecular assays to identify apoptosis such as TUNEL, which may be more sensitive

death, linking it to one specific molecular mechanism when there are likely multiple forms of cell death occurring. The above diverse response between C-Frag, apoptosis, and various drugs that induce ER stress suggests an interchangeable relationship among types of cell death, prompting further study of the relationships between various mechanisms and different types of cell death (Table 1).

Heterogeneity of cell death types. HCT116 cells were treated with various combinations of drugs at various concentrations. The type of cell death incurred was scored by cytogenomic analysis where C-Frag and apoptosis are distinguishable (Table 1 and Figures 4a and b). Although the occurrence of apoptosis during mitosis has not been

established, a general lack of morphological descriptions of mitotic apoptosis suggests that it may not occur. It is noteworthy that apoptotic cells can be detected in populations where C-Frag is the primary form of cell death, and vice versa. For individual cells, cell death is an occurrence of opportunity, and the form of cell death is contingent on the genome status and environmental conditions.

Cell death type is influenced by dosage of drug treatment. Effects of drug concentration on death type were examined, as the required dosage for inducing apoptosis is often higher than what is clinically obtainable.[8,26] For colcemid-based combinations of treatments, Dox at 10 and 1 μg/ml potently, but to different degrees, induces C-Frag. Mitomycin-C (MMC) treatment at 10 μg/ml is also capable of increasing the frequencies of C-Frag, whereas 1 μg/ml MMC, and 10 and 1 μg/ml methotrexate (MTX) treatment do not induce C-Frag at appreciable levels. Surprisingly, none of these treatments induced more than 2% apoptosis, based on morphological analysis suggesting that in this *in vitro* cancer system, C-Frag is the major form of cell death. The lack of apoptosis could be because of the length of treatment, as 6 h of treatment may be insufficient to induce late-stage apoptosis where apoptotic cells are identifiable by morphology.

In the case of docetaxel and Dox combinatorial treatments, a high concentration (10 μM) of docetaxel combined with 1 μg/ml Dox increased the apoptotic response, whereas low concentrations (1 μM) of docetaxel and 1 μg/ml Dox primarily resulted in cell death by C-Frag (Figure 4b). Although the observed levels of cell death are often less than 5%, this number represents the population as a whole, the majority of which is non-mitotic. The majority of the mitotic cells are therefore undergoing C-Frag. Similarly, treatment with low concentrations of Dox and 100 nM 17-DMAG primarily results in cell death through C-Frag; however, at increased doses of Dox apoptosis increases (Figure 3g).

C-Frag is linked to increased proteasomal activity. The H1299-v138 cell line contains a temperature-sensitive p53 mutation.[9] Shifting these cells from 39 to 32 °C results in C-Frag.[9] To establish the relationship between different types of cell death, proteasome activity was measured at day 0 (restrictive temperature) until day 3 (days 1–3, permissive temperature) over which time the majority of cell death takes place. From day 0 to day 2 proteasome activity increased 1.79-fold. Proteasomal activity correlates with the induction of C-Frag ($r^2 = 0.768$), showing that induction of C-Frag is also linked to a major mechanism of protein degradation, which is strongly associated with cell death.[27]

Discussion

C-Frag is a stress response. C-Frag is a general response to diverse stress. The association of C-Frag with broad-ranging factors suggests that the dynamics of a complex system is not likely explained by only one specific molecular mechanism. The concept presented here finally solves a mystery of the phenomenon of chromosome pulverization.

For decades, the mechanism of chromosome pulverization has been linked to various specific causative factors such as viral vaccination, defective genes, and environmental challenges.[28–31] C-Frag (erroneously termed premature chromosome condensation (PCC)) has been linked exclusively to single molecular mechanisms without the realization that induction of MCD is a common response to stress.[20] This current study shows that the underlying general cause of this long observed phenomenon is system stress rather than a specific gene-associated phenomenon (Table 2). This conclusion also shows that multiple response pathways should be monitored in other apoptosis and molecular pathway research.

The stress–C-Frag link is significant. Stress is a major driver of genomic instability-mediated cancer evolution.[1] Genome change occurs as an adaptive response to stress, increasing population diversity, the probability of survival, and potentially the acquisition of new features essential for cancer progression and drug resistance. Recently, examples of extreme genome change (genome chaos) within tumors have been reported, where multiple intra- and inter-region arrangements of chromosomes occur.[11,14,15] It has been suggested that these events are the result of local chromosome shattering,[14,15] although C-Frag could function as a necessary step. C-Frag has been shown to occur in one or a small number of chromosomes,[9] which reconciles why only a limited number of chromosomes can be involved in cases of genome chaos. We have also observed genome chaos in multiple cell lines in

Table 2 Diverse mechanisms of C-Frag

	References
Specific mechanism of C-Frag	
Caffeine uncoupling of the cell cycle	40
Chromosome-localized UV damage	30
Loss of ATM function	Current study
Loss of ATR function	28
Loss of p53 function	29
Measles vaccination	41
Stresses	
Calcium	Current study
Genomic instability	Current study
HSP inhibition	Current study; 23
Oxidative	Current study
Temperature change	Current study; 23, 31
Unfolded protein response	Current study
Drugs	
Arsenic trioxide	23, 31
Cytosine arabinoside	Current study
Colcemid	9
Docetaxel	Current study
Doxorubicin	9
Methotrexate	9
Mitomycin-C	Current study
Pathological conditions	
Breast cancer	Current study
Brain malignancies	Current study
Hematological malignancies	Current study
Lipoma	Current study
Leukocytosis	Current study
Mitotic components	
Centrosome amplification	Current study

response to stress (Heng *et al.*, unpublished results). As C-Frag is linked to stress, it is likely that these two events occur together.

C-Frag and centrosome amplification. As C-Frag occurs at mitosis, it is ideal to search for the mechanism leading to it within this time window. Centrosome amplification often results in multi-polar divisions, which can cause aneuploidy or can result in cell death.[32] Heat shock or inhibition of HSP activity can induce MCD consequent to centrosome amplification.[23,31,33] HSP90 induction can be linked to broad stressors such as temperature shift and chemotherapeutics, as it is a core component of the centrosome that functions in a number of pathways, including the Chk1 pathway, which has a central role in the G_2 checkpoint. Ablation of HSP90 function increases the mitotic index and cell death during mitosis, largely by C-Frag, while correlating with increased centrosome amplification, suggesting a direct link between stress, centrosome amplification, and C-Frag. Furthermore, centrosome amplification has also been linked to wound healing, development of polyploid liver cells, genomic instability, and cancer.[32] These responses can also be linked to C-Frag; thus, we conclude that C-Frag simply represents one of the main phenotypes of cells that have undergone 'cell death occurring during metaphase'.[9,34]

We now propose a general model of C-Frag. Various cellular stresses can act on the mitotic machinery, such as the centrosome, and abnormal function of mitotic systems leads to C-Frag. In other words, centrosome amplification-induced mitotic failure leads to a C-Frag phenotype. As centrosomes represent major parts of the mitotic machinery, we anticipate that other important components of mitosis could also be responsible for subtypes of cell death.[13] Inhibition of HSP90 reinforces these results as HSP90 has a pivotal role in centrosome stability, and its inhibition leads to increased C-Frag.

Potential diagnostic and prognostic uses of C-Frag. One problem with the use of apoptosis in disease treatment has been the observation that drug concentrations that often induce apoptosis in experimental systems do not seem to induce apoptosis in clinical settings, unless much higher concentrations are used.[8] Our study shows that C-Frag can account for a portion of this disparity. Another important finding is the link between elevated C-Frag frequency and various disease conditions. C-Frag was shown to occur broadly across many types of tumors, underscoring that C-Frag is not a cell line- or gene-specific phenomenon, but rather a general response that is influenced by pathological stress to eliminate cells and maintain system stability. Further clinical investigation is needed to link elevated C-Frag to specific clinical conditions.

Induction of a specific type of cell death is largely dependent on convenience. Our data suggest that cell death is a highly complex process, and multiple forms of cell death result from a simple response to overwhelming stress(es). Whenever a population of cells is stressed sufficiently to induce death, it is likely that more than one type of cell death will be induced owing to the heterogeneous
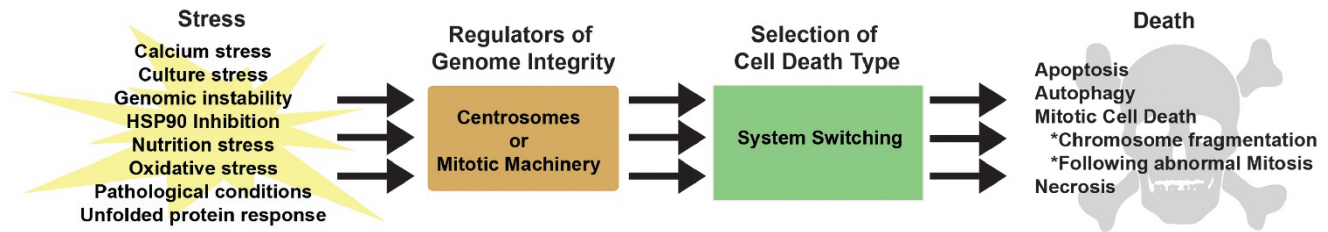
Figure 5 A proposed model illustrating the relationship between stress and the induction of various types of cell death. When a cell faces a given stress that is strong enough to induce death, multiple factors influence the selection of the specific pathways of cell death and depend on the availability of targets (mitotic or interphase cells) and/or the availability of certain pathways

means of eliminating unwanted cells. One specific form of cell death may dominate in specific instances, although sub-populations will likely undergo other terminal fates. The cell death type is highly dependent on multiple factors, including the original cell population, the type and amount of stress incurred, and the availability of targets. For instance, cancer cells are highly mitotic as compared with normal somatic cells, making mitotic cells an increasingly likely target. Unfortunately, common molecular methods such as western blotting only identify changes in an admixture of cells, but do not show variation on the single-cell level. Echoing other reports, our results showing cell death heterogeneity underscore the importance of individual cell-based analyses.[1,8,12,35]

Following the demonstration that the different tested stressors can induce C-Frag, it was determined that system stress represents the general mechanisms of C-Frag. The approach here differs from traditional approaches where a specific molecular pathway is identified in order to study a mechanism. However, for any given complex system, general mechanisms can be understood using the synthesis of the large number of specific mechanisms.[1,12] Further synthesis led us to conclude that stress can induce all types of cell death and that stress is not specific for C-Frag. Such a conclusion complements the traditional approaches of cell death research that focus on specific molecular pathways.

To illustrate the general mechanism of cell death, we present a model suggesting a link between diverse molecular mechanisms, maintenance of genome integrity, system stress, and various types of cell death (Figure 5). This is similar to the relationship between the evolutionary mechanism of cancer and all individual molecular mechanisms.[1,19] All individual molecular mechanisms can be linked to system stress in a stochastic manner. The relationship above illustrated between system stress, C-Frag, cell death, and genome alteration shows a portion of the complex means for maintaining genome stability and yet creating new genomes, which fits well within the system biology concept where system dynamics and stability can be achieved through vastly different individual molecular mechanisms. Knowing that various types of cell death can be induced by stress and coexist within heterogeneous cell populations, it is not surprising to identify the association between C-Frag and other forms of cell death. It is also possible that C-Frag can be linked to apoptosis or/and autophagy under certain conditions in terms of specific molecular pathways. However, C-Frag represents an independent form of MCD.

It should be pointed out that certain types of cell death tend to dominate in a given analysis. This is because of system complexity and high levels of cellular heterogeneity affecting cell death selection, and may help explain many of the inconsistencies of MCD. For instance, in some cases it has been shown contrastingly to be both caspase-dependent and -independent.[9,31,36,37] It is quite possible that C-Frag and other subtypes of MCD coexist, and some subtypes can be linked to caspase activity. In our system, we have monitored a defined window of mitosis based on cytogenomic analysis, reducing the chance of including other types of cell death when scoring C-Frag. Moreover, the different systems examined show different pathways that can all lead to MCD. Finally, C-Frag represents a powerful means to create a new system during crises stages of somatic evolution.[38]

Materials and Methods

Cell culture. Cell lines were grown in RPMI-1640 (Hyclone, South Logan, UT, USA) media supplemented with 10% fetal bovine serum (FBS) (Hyclone) in 5% CO_2 at 37°C unless otherwise noted. HCT116 14-3-3$\sigma^{-/-}$, H460, and H1299-v138 cells were grown with 400 μg/ml G418 (Fisher Scientific, Pittsburgh, PA, USA). The cell lines used in the following experiments were chosen because of their genetic manipulations. The cell lines that have not been modified were selected as they are not abnormally prone or resistant to C-Frag. Their identity was confirmed by spectral karyotyping within 6 months of use (Supplementary Table S1). The HCT116, H1299-v138, and COLO-357 cell lines were provided by Drs. Bert Vogelstein, Yi Sun, and Anton Goustin, respectively.

Isolation of cells from mouse tumors. Following resection, tumors were minced finely in PBS. Visible chunks of tumor were then digested in a trypsin solution (Hyclone) and drawn through a 25G needle until chunks were separated. The trypsin was then quenched with FBS and the two portions of the cells were mixed back together and forced through a 30-μm nylon screen to remove any remaining clumps.

Chromosome preparation from cell lines, cultured lymphocytes, and solid tumors. Cytogenomic preparation performed as described by Ye *et al.*[13] Briefly, cells were harvested, pelleted, suspended in 0.4% KCl for 20 min at 37°C, fixed in 3 : 1 methanol:acetic acid, and dropped onto ice-cold glass slides. The slides were then stained for 15 min at room temperature in 2% Giemsa solution.

Slide scoring. Slides were scored for C-Frag as described previously;[9] briefly, mitotic figures were observed and cells with chromosomal degradation consistent to what was previously scored as C-Frag were counted.[9] For treatments where the CFI was shown, only mitotic cells were scored. CFI was calculated by dividing the number of cells undergoing C-Frag by the total number of mitotic cells counted.

Western blotting. Western blotting analysis was performed as described by Xu *et al.*[39] To determine expression levels of CHOP, KDEL, XBP1 and α-tubulin total cell lysates were prepared from treated COLO-357 cells using NP-40 lysis buffer (1% NP-40, 50 mM Tris-HCL pH 7.5, 150 mM NaCl, 0.05% SDS, 0.5 mM Na vanadate, 100 mM NaF, 50 mM β-glycerophosphate, and 1 mM

phenylmethylsulfonyl fluoride) supplemented with protease inhibitors (EDTA-free Complete Mini, Roche, San Francisco, CA, USA). Denatured proteins were separated by SDS-PAGE on 10% Tris-glycine polyacrylamide gels and transferred to a 0.45 mm PVDF membrane (GE Healthcare, Waukesha, WI, USA). Detection was performed with CHOP (Santa Cruz Biotech, Santa Cruz, CA, USA), KDEL (Enzo Life Sciences, Plymouth Meeting, PA, USA), XBP1 (Santa Cruz Biotech) and α-tubulin (Sigma-Aldrich, St Louis, MO, USA) antibodies at manufacturers suggested concentrations. HRP conjugated Rabbit TrueBlot secondary antibody (eBioscience, San Diego, CA, USA) was used for secondary diction as is avoids detecting the Ig heavy and light chains from denatured samples. Bound antibody was detected using enhanced chemiluminescence (ECL) reagent or ECL Plus reagent (GE Healthcare) according to the manufacturer's protocol.

Induction of MC. MC was induced as described by Chan et al.[17] HCT116 14-3-3$\sigma^{-/-}$ cells were treated for up to 72 h with 0.2 μg/ml Dox, photographed, harvested, and subjected to cytogenetic preparation and analysis at the indicated intervals.

Abrogation of G$_2$ checkpoint by UCN-01 treatment. HCT116 cells were treated concurrently with 1 μg/ml Dox and 300 nM UCN-01 (Sigma-Aldrich) for 6 h.

Normoxic treatment. HCT116 cells were grown in a hypoxic chamber with 3.5% O$_2$ and 5% CO$_2$, and acclimatized for 5 days until cells were actively dividing. The cells were then pretreated for 3 h with colcemid, a mitotic shake-off was performed, and the cells were treated for 6 or 12 h with 1 μg/ml Dox under colcemid pressure.

Temperature shift. COLO-357 cells were cultured at 37°C and then cultured at 42°C for 10 days at which time cells stabilized and began to grow again. The cells were then transferred back to 37°C and harvested at the indicated time points (Figures 3a and b).

Linking C-Frag and genomic instability. MDAH-041 and MOSEC cells were harvested during different time periods where the population showed genome stability and instability as determined by spectral karyotyping (SKY), and prepared for cytogenomic evaluation.[11,13]

Induction of pathway-defined stress. COLO-357 cells were treated three independent times for 4, 8, and 24 h with the ER stress inducers A23187, DTT, TG, and TM (Sigma-Aldrich).

Centrosome amplification. Cells were attached to glass slides using a Shandon Cytospin at 1000 r.p.m. for 5 min, fixed for 7 min in 1% paraformaldehyde, permeabilized with 0.1% Triton X-100, incubated with a γ-tubulin antibody (Abcam, Cambridge, MA, USA), washed, incubated with an Alexa-Fluor-488-labeled anti-mouse antibody (Invitrogen, Carlsbad, CA, USA), washed, coverslipped with DAPI and anti-fade (Invitrogen), and imaged.

Inhibition of HSP90. HCT116 cells were treated for a total of 54 h with Dox (50 nM, 150 nM, 1 μM, or 1 μg/ml); after 24 h of treatment, 100 nM 17-DMAG (LC Laboratories, Woburn, MA, USA) was added to the cells. Following a 24-h incubation of 17-DMAG and Dox, 1 × colcemid was added for 6 h prior to harvest.

Proteasomal activity assay. Proteosomal activity was measured as previously described.[33] Cells were washed 3 times with ice-cold PBS and scraped for centrifugation. Cell pellets were resuspended in lysis buffer (50 mM Tris-Cl, pH 7.5, 10 mM MgCl$_2$, 100 mM KCl, 1% Triton X-100, 10% glycerol, 1 mM DTT, 1X protease inhibitor cocktail) and mixed with rotation at 4°C for 2 h. Extract was centrifuged at 13 200 rpm for 10 min at 4°C. Protein concentration was determined using Bradford Assay Kit (Bio-Rad, Hercules, CA, USA). Chymotrypsin-like activity of the 20S proteasome was measured by incubation of 40 μM Suc-Leu-Leu-Val-Tyr-AMC (Boston BioChem, Cambridge, MA, USA) with 20 μg cell extract in 100 μl assay buffer (50 mM Tris-Cl, pH 7.5) at 37°C for 1 h. The released fluorescence signals were monitored with an excitation filter of 355 nm and an emission filter of 460 nm using VersaFluot Fluorometer (Bio-Rad).

Differential induction of apoptosis and C-Frag. HCT116 cells were treated for 6 and 12 h with 1 μg/ml Dox (MP Biochemicals, Solon, OH, USA), 1 μM docetaxel (MP Biochemicals), 10 μM docetaxel, and 1 or 10 μM docetaxel combined with 1 μg/ml Dox.

Statistical analysis. Paired t-tests were performed using Microsoft Excel.

1. Heng HH, Stevens JB, Bremer SW, Ye KJ, Liu G, Ye CJ. The evolutionary mechanism of cancer. *J Cell Biochem* 2010; **109**: 1072–1084.
2. Negrini S, Gorgoulis VG, Halazonetis TD. Genomic instability – an evolving hallmark of cancer. *Nat Rev Mol Cell Biol* 2010; **11**: 220–228.
3. Tabas I, Ron D. Integrating the mechanisms of apoptosis induced by endoplasmic reticulum stress. *Nat Cell Biol* 2011; **13**: 184–190.
4. Brown JM, Wouters BG. Apoptosis, p53, and tumor cell sensitivity to anticancer agents. *Cancer Res* 1999; **59**: 1391–1399.
5. Park SS, Kim MA, Eom Y-W, Choi KS. Bcl-xL blocks high dose doxorubicin-induced apoptosis but not low dose doxorubicin-induced cell death through mitotic catastrophe. *Biochem Biophys Res Commun* 2007; **363**: 1044–1049.
6. Blagosklonny MV. Apoptosis, proliferation, differentiation: in search of the order. *Semin Cancer Biol* 2003; **13**: 97–105.
7. Kondo S. Altruistic cell death: mitotic catastrophe model of apoptosis. *Protein Nucleic Acid Enzyme* 1994; **39**: 2238–2245.
8. Roninson IB, Broude EV, Chang BD. If not apoptosis, then what? – Treatment-induced senescence and mitotic catastrophe in tumor cells. *Drug Resist Updat* 2001; **4**: 303–313.
9. Stevens JB, Liu G, Bremer SW, Ye KJ, Xu W, Xu J et al. Mitotic cell death by chromosome fragmentation. *Cancer Res* 2007; **67**: 7686–7694.
10. Castedo M, Perfettini JL, Roumier T, Kroemer G. Cyclin-dependent kinase-1: linking apoptosis to cell cycle and mitotic catastrophe. *Cell Death Differ* 2002; **9**: 1287–1293.
11. Heng HH, Stevens JB, Liu G, Bremer SW, Ye KJ, Reddy PV et al. Stochastic cancer progression driven by non-clonal chromosome aberrations. *J Cell Physiol* 2006; **208**: 461–472.
12. Heng HH, Bremer SW, Stevens JB, Ye KJ, Liu G, Ye CJ. Genetic and epigenetic heterogeneity in cancer: a genome-centric perspective. *J Cell Physiol* 2009; **220**: 538–547.
13. Ye CJ, Stevens JB, Liu G, Bremer SW, Jaiswal AS, Ye KJ et al. Genome based cell population heterogeneity promotes tumorigenicity: the evolutionary mechanism of cancer. *J Cell Physiol* 2009; **219**: 288–300.
14. Berger MF, Lawrence MS, Demichelis F, Drier Y, Cibulskis K, Sivachenko AY et al. The genomic complexity of primary human prostate cancer. *Nature* 2011; **470**: 214–220.
15. Stephens PJ, Greenman CD, Fu B, Yang F, Bignell GR, Mudie LJ et al. Massive genomic rearrangement acquired in a single catastrophic event during cancer development. *Cell* 2011; **144**: 27–40.
16. Borst P, Rottenberg S. Cancer cell death by programmed necrosis? *Drug Resist Updat* 2004; **7**: 321–324.
17. Chan TA, Hermeking H, Lengauer C, Kinzler KW, Vogelstein B. 14-3-3σ is required to prevent mitotic catastrophe after DNA damage. *Nature* 1999; **401**: 616–620.
18. Tse AN, Schwartz GK. Potentiation of cytotoxicity of topoisomerase I poison by concurrent and sequential treatment with the checkpoint inhibitor UCN-01 involves disparate mechanisms resulting in either p53-independent clonogenic suppression or p53-dependent mitotic catastrophe. *Cancer Res* 2004; **64**: 6635–6644.
19. Heng HH. The genome-centric concept: resynthesis of evolutionary theory. *Bioessays* 2009; **31**: 512–525.
20. Stevens JB, Abdallah BY, Regan SM, Liu G, Bremer SW, Ye CJ et al. Comparison of mitotic cell death by chromosome fragmentation to premature chromosome condensation. *Mol Cytogenet* 2010; **3**: 20.
21. Massabuau JC. From low arterial- to low tissue-oxygenation strategy. An evolutionary theory. *Respir Physiol* 2001; **128**: 249–261.
22. Zhang K, Kaufman RJ. From endoplasmic-reticulum stress to the inflammatory response. *Nature* 2008; **454**: 455–462.
23. Taylor BF, McNeely SC, Miller HL, States JC. Arsenite-induced mitotic death involves stress response and is independent of tubulin polymerization. *Toxicol Appl Pharmacol* 2008; **230**: 235–246.
24. Shen K, Wang Y, Brooks S, Raz A, Wang YA. ATM is activated by mitotic stress and suppresses centrosome amplification in primary but not in tumor cells. *J Cell Biochem* 2006; **99**: 1267–1274.

25. Lange BMH, Bachi A, Wilm M, Gonzalez C. Hsp90 is a core centrosomal component and is required at different stages of the centrosome cycle in *Drosophila* and vertebrates. *EMBO J* 2000; **19**: 1252–1262.

26. Janssen A, Kops GJPL, Medema RH. Elevating the frequency of chromosome mis-segregation as a strategy to kill tumor cells. *Proc Natl Acad Sci USA* 2009; **106**: 19108–19113.

27. Korolchuk VI, Menzies FM, Rubinsztein DC. Mechanisms of cross-talk between the ubiquitin–proteasome and autophagy–lysosome systems. *FEBS Lett* 2010; **584**: 1393–1398.

28. Brown EJ, Baltimore D. ATR disruption leads to chromosomal fragmentation and early embryonic lethality. *Genes Dev* 2000; **14**: 397–402.

29. Fukasawa K, Wiener F, VandeWoude GF, Mai SB. Genomic instability and apoptosis are frequent in p53 deficient young mice. *Oncogene* 1997; **15**: 1295–1302.

30. Hübner B, Strickfaden H, Müller S, Cremer M, Cremer T. Chromosome shattering: a mitotic catastrophe due to chromosome condensation failure. *Eur Biophys J* 2009; **38**: 729–747.

31. Taylor BF, McNeely SC, Miller HL, Lehmann GM, McCabe Jr MJ, States JC. p53 suppression of arsenite-induced mitotic catastrophe is mediated by p21CIP1/WAF1. *J Pharmacol Exp Ther* 2006; **318**: 142–151.

32. Godinho S, Kwon M, Pellman D. Centrosomes and cancer: how cancer cells divide with too many centrosomes. *Cancer Metastasis Rev* 2009; **28**: 85–98.

33. Xu H, Ju D, Jarois T, Xie Y. Diminished feedback regulation of proteasome expression and resistance to proteasome inhibitors in breast cancer cells. *Breast Cancer Res Treat* 2008; **107**: 267–274.

34. Kroemer G, El-Deiry WS, Golstein P, Peter ME, Vaux D, Vandenabeele P *et al.* Classification of cell death: recommendations of the Nomenclature Committee on Cell Death. *Cell Death Differ* 2005; **12** (S2): 1463–1467.

35. Carmona-Gutierrez D, Eisenberg T, Büttner S, Meisinger C, Kroemer G, Madeo F. Apoptosis in yeast: triggers, pathways, subroutines. *Cell Death Differ* 2010; **17**: 763–773.

36. Niikura Y, Ogi H, Kikuchi K, Kitagawa K. BUB3 that dissociates from BUB1 activates caspase-independent mitotic death (CIMD). *Cell Death Differ* 2010; **17**: 1011–1024.

37. O'Sullivan-Coyne G, O'Sullivan GC, O'Donovan TR, Piwocka K, McKenna SL. Curcumin induces apoptosis-independent death in oesophageal cancer cells. *Br J Cancer* 2009; **101**: 1585–1595.

38. Heng HH, Liu G, Stevens JB, Bremer SW, Ye KJ, Abdallah BY *et al.* Decoding the genome beyond sequencing: the new phase of genomic research. *Genomics* 2011; doi:10.1016/j.ygeno.2011.05.008 (in press).

39. Xu J, Zhou J-Y, Tainsky MA, Wu GS. Evidence that tumor necrosis factor-related apoptosis-inducing ligand induction by 5-aza-2′-deoxycytidine sensitizes human breast cancer cells to adriamycin. *Cancer Res* 2007; **67**: 1203–1211.

40. Schlegel R, Pardee AB. Caffeine-induced uncoupling of mitosis from the completion of DNA replication in mammalian cells. *Science* 1986; **232**: 1264–1266.

41. Nichols WW, Levan A. Measles associated chromosome breakage. *Archiv fèur die gesamte Virusforschung* 1965; **16**: 168–174.

Supplementary Information accompanies the paper on Cell Death and Disease website (http://www.nature.com/cddis)